JEE Journal of Ecological Engineering

Journal of Ecological Engineering, 2027, 28(1), 128–143
https://doi.org/10.12911/22998993/241649
ISSN 2299–8993, License CC-BY 4.0

Received: 2026.09.25
Accepted: 2026.11.16
Published: 2026.12.01

Nitrogen pathways in sequencing batch reactors with floating biofilm carriers treating dairy wastewater – a dynamic activated sludge model tested against independent data

Ihor Kobylko[1*]

[1] Department of Water Supply, Water Disposal and Drilling Engineering, National University of Water and Environmental Engineering, Soborna St. 11, 33028 Rivne, Ukraine
E-mail: i.v.kobylko@nuwm.edu.ua

ABSTRACT

Sequencing batch reactors (SBRs) with floating biofilm carriers are a promising option for small dairy plants, because nitrification and denitrification can proceed simultaneously in one reactor at a low dissolved oxygen (DO) concentration. Total nitrogen (TN) removal alone, however, does not show how much nitrogen is converted to N_2 and how much leaves with the excess sludge. To assess these pathways, a dynamic model based on Activated Sludge Model No. 3 was developed, with two-step nitrification, limited substrate storage, apparent oxygen half-saturation constants for simultaneous nitrification–denitrification in flocs and a lumped biofilm limited by the carrier surface. Nitrogen and COD balances agreed to within 0.003%. The model was checked against two experimental studies published by other groups; both used synthetic wastewater, so this validation is preliminary. After two apparent constants were calibrated on a DO series in a continuous hybrid reactor, the model reproduced TN removal at C/N 8–10 without further calibration (RMSE 5.7 percentage points), but not at C/N 4 or at low DO, where nitrification in the real reactor was impaired. For an aerated moving-bed SBR it reproduced the sludge concentration (within 3–12%) and end-of-cycle nitrate at COD/N 10 but overestimated nitrification. Scenario simulations for dairy wastewater (COD 2000 mg/L, sludge age 15 d) showed that the share of nitrogen removed with the excess sludge increases from about 12% at COD/N 10 to 58% at COD/N 45, while the share converted to N_2 decreases accordingly. Carriers had almost no effect on overall TN removal with the literature nitrification kinetics but at COD/N $\geq$ 30 reduced the share of nitrogen bound in the sludge. When nitrifier growth rates were lowered so that the simulated residual ammonium approached the measured values, the share of nitrogen in the sludge changed by at most 2.2 percentage points. Without carriers, however, nitrifiers washed out at DO $\leq$ 1 mg/L and most of the remaining nitrogen left as effluent ammonium instead of N_2; with carriers nitrification was maintained at DO 1 mg/L. For dairy wastewater rich in organic matter, TN removal alone therefore cannot show which part of the nitrogen was actually denitrified.

Keywords: simultaneous nitrification–denitrification, sequencing batch reactor, floating biofilm carriers, activated sludge model, dairy wastewater, nitrogen assimilation, nitrogen transformation.

INTRODUCTION

Wastewater from dairy processing is usually warm, high in organic matter and highly variable in composition over a working day. Most of the organic load comes from lactose, milk proteins and fats, so COD can range from about 1 to several grams per litre. Total nitrogen in such effluents is initially present mainly in organic form, and its concentration depends on the type of products and on how much milk enters the drainage system (Ahmad et al., 2019; Kolev Slavov, 2017).

Many small and medium-sized dairy plants in Eastern Europe still discharge their production wastewater to the municipal sewer with practically no pretreatment apart from fat removal. Another common arrangement is a small treatment plant shared by the dairy and the local

community. In such cases the treatment plant can be quite sensitive even to minor changes in the dairy's operating regime (Zawadzka et al., 2021). Stricter requirements for nitrogen compounds make compact on-site biological treatment at the plant itself increasingly relevant.

Sequencing batch reactors (SBRs) are well suited to these conditions. They can operate under variable flow and load, allow the main processes to be carried out in a single tank, and the duration and sequence of the cycle phases can be changed without rebuilding the plant. If a low dissolved oxygen concentration is maintained during aeration, nitrification and denitrification can take place at the same time in the same reactor. This process is called simultaneous nitrification–denitrification (SND).

The mechanism of SND is related to the uneven distribution of oxygen inside activated sludge flocs or biofilm. In the outer layer, which receives oxygen directly from the water, aerobic conditions develop and ammonium nitrogen is oxidised. In the inner part of the floc or biofilm there is not enough oxygen, so anoxic conditions can form there, favourable for the reduction of nitrate and nitrite coming from the outer layer (Pochana and Keller, 1999). Intracellular storage of organic substrate can play an additional role. Polyhydroxyalkanoates accumulated during a period of excess organic matter can serve as electron donors after the soluble COD in the water has been exhausted (Third et al., 2003).

It is, however, quite difficult to predict in advance how effective SND will be at a particular plant. Pilot-scale installations operated at low dissolved oxygen achieved stable nitrogen removal (Keene et al., 2017). In studies with granular activated sludge treating municipal wastewater, on the other hand, SND remained limited even with large granules (Layer et al., 2020). The use of biofilm carriers in an SBR makes it possible to increase the anoxic volume and to retain slow-growing nitrifying microorganisms regardless of the rate at which activated sludge is wasted (Ødegaard, 2006). Laboratory and full-scale studies indicate that carriers in a number of cases give higher total nitrogen removal than systems without them (Jin et al., 2023; Zhang et al., 2024). The effect, however, depends both on the properties of the carrier and on the C/N ratio of the wastewater (Iannacone et al., 2019; Li et al., 2019).

Mathematical modelling of such systems faces at least two important difficulties. The first concerns the description of SND itself. The IWA family of activated sludge models describes the main processes in the reactor volume well (Henze et al., 2015), and several ways of describing two-step nitrification on the basis of ASM3 have been proposed (Iacopozzi et al., 2007; Kaelin et al., 2009). There are also detailed one-dimensional biofilm models that account for diffusion and biochemical reactions together (IWA Task Group on Biofilm Modeling, 2015). Such models have been combined with activated sludge models to describe hybrid biological reactors (Boltz et al., 2009).

Detailed biofilm models, however, require a large number of parameters that are practically never determined in real projects or at full-scale plants. A simpler approach is therefore to treat the reactor as completely mixed and to use apparent oxygen half-saturation constants that account, in a lumped way, for diffusion inside flocs or cell clusters. These apparent constants are usually higher than the intrinsic kinetic values and depend on floc size, mixing conditions and loading (Arnaldos et al., 2015; Picioreanu et al., 2016). For this reason they generally have to be determined separately for each system.

The second problem concerns the fate of the removed nitrogen. In wastewater with a high content of organic matter, a considerable part of the nitrogen that disappears from the liquid phase can be incorporated into new biomass and removed with the excess activated sludge. TN removal efficiency determined only from the difference between inlet and outlet concentrations therefore cannot distinguish nitrogen denitrified to N_2 gas from nitrogen removed with the biomass. The nitrogen demand of activated sludge is well known in design practice (Metcalf & Eddy, Inc. et al., 2014). When the COD/N ratio is too high, nitrogen deficiency can, among other things, impair sludge properties and cause bulking (Guo et al., 2014). Yet the share of nitrogen that passes into biomass is not always determined separately from the overall TN removal figure. For dairy wastewater this problem is particularly relevant, because the COD/N ratio can exceed 30. In that case separating the nitrogen flows matters both for interpreting experimental results correctly and for judging whether biofilm carriers and dissolved oxygen control are worthwhile.

An earlier version of the model and the results of a local sensitivity analysis were published in Kobylko (2026). In the present work the model has been developed in three main directions. First, biomass is described fully dynamically:

its growth, endogenous respiration, the return of nitrogen on decay and the wasting of activated sludge according to the set sludge retention time (SRT) are all included. Second, storage of organic substrate is described according to the ASM3 concept, with a limited storage capacity. Third, biomass attached to the carriers is described separately, with its amount limited by the available carrier surface.

The main aim was to check whether such a model, in which only two apparent oxygen constants are adjusted, can adequately describe published experimental data that were not used to build it. If so, the model can be used to address a practical question: in an SBR treating dairy wastewater, how is nitrogen distributed between its three main routes – conversion to N_2 gas, removal with the excess sludge and what remains in the treated water – across the range of COD/N ratios typical of these effluents?

MATERIALS AND METHODS

Model structure

The structure of the model is summarised in Figure 1. It follows the component and process structure of Activated Sludge Model No. 3 (Gujer et al., 1999). The liquid phase contains dissolved oxygen S_O, readily biodegradable substrate S_S, ammonium S_{NH}, nitrite S_{NO2}, nitrate S_{NO3} and dinitrogen S_{N2} (the last one only for bookkeeping), together with slowly biodegradable substrate X_S, heterotrophic biomass X_H, internal storage products X_{STO}, ammonia-oxidising bacteria X_{AOB}, nitrite-oxidising bacteria X_{NOB} and inert particulate matter X_I. Attached biomass on the carriers is described by five further states ($X_{f,H}$, $X_{f,STO}$, $X_{f,AOB}$, $X_{f,NOB}$, $X_{f,I}$), expressed per litre of reactor volume. All organic states are in mg COD/L and nitrogen states in mg N/L.

Heterotrophs take up S_S into X_{STO} under aerobic or anoxic conditions and grow on the stored material, as in ASM3. In reality storage and growth compete for the substrate and the storage pool cannot grow without limit (Sin et al., 2005). The simplest way to express this, used earlier for bulking control (Makinia et al., 2006), is to slow storage as the cell becomes saturated:

$$\rho_{STO} = k_{STO} \cdot S_S/(K_S + S_S) \cdot S_O/(K_O + S_O) \cdot \cdot \max(0, 1 - (X_{STO}/X_H)/f_{STO,max}) \cdot X_H \quad (1)$$

where: $f_{STO,max} \to \infty$ Equation (1) reduces to the original ASM3 rate.

Growth on stored products requires ammonium as a nutrient (half-saturation constant $K_{NH,H}$ = 0.01 mg N/L), and every gram of new biomass removes $i_{N,BM}$ = 0.07 g N from solution. Endogenous respiration converts active biomass into X_I and returns the difference in nitrogen content, $i_{N,BM} - f_I \cdot i_{N,XI}$, to the ammonium pool. This last term is what makes the difference between gross and net assimilation: at an SRT of 10–15 d most of the biomass grown during a cycle decays inside the reactor, and only the nitrogen contained in the wasted sludge is removed from the system.

Nitrification is split into nitritation by AOB and nitratation by NOB, following the two-step extension of ASM3 by Iacopozzi et al. (2007), which was also reduced to a compact form for SBRs by Cruz Bournazou et al. (2012); a comparable structure with separate nitrite steps is used in ASMN (Hiatt and Grady, 2008):

$$\rho_{AOB} = \mu_{AOB} \cdot S_{NH}/(K_{NH,AOB} + S_{NH}) \cdot \cdot S_O/(K_{O,AOB} + S_O) \cdot X_{AOB} \quad (2)$$

$$\rho_{NOB} = \mu_{NOB} \cdot S_{NO2}/(K_{NO2,NOB} + S_{NO2}) \cdot \cdot S_O/(K_{O,NOB} + S_O) \cdot X_{NOB} \quad (3)$$

Heterotrophs reduce both nitrate and nitrite to N_2. The electron flow available for anoxic storage, growth and respiration is shared between the two acceptors in proportion to their concentrations, with 2.86 g COD per g NO_3-N and 1.71 g COD per g NO_2-N. Allowing direct reduction of nitrite (the nitrite shunt) matters in simulations of this kind: if nitrate is reduced only to nitrite, the nitrite is immediately re-oxidised by NOB in the aerated bulk and very little N_2 is formed, an artificial loop that is easy to miss when only TN is checked.

Simultaneous nitrification–denitrification in the suspended flocs is represented through apparent constants. All anoxic heterotrophic processes are multiplied by an inhibition term $K_{O,anox}/(K_{O,anox} + S_O)$. In standard ASM3 this constant equals the aerobic K_O (0.2 mg/L), which practically switches off denitrification above 1 mg/L. A larger apparent value lets part of the floc remain anoxic at moderate bulk DO, which is the usual way of describing SND in completely mixed models (Arnaldos et al., 2015). The apparent constant $K_{O,AOB}$ plays the same role for nitrifiers, whose oxygen supply inside a floc is reduced by heterotrophic consumption in

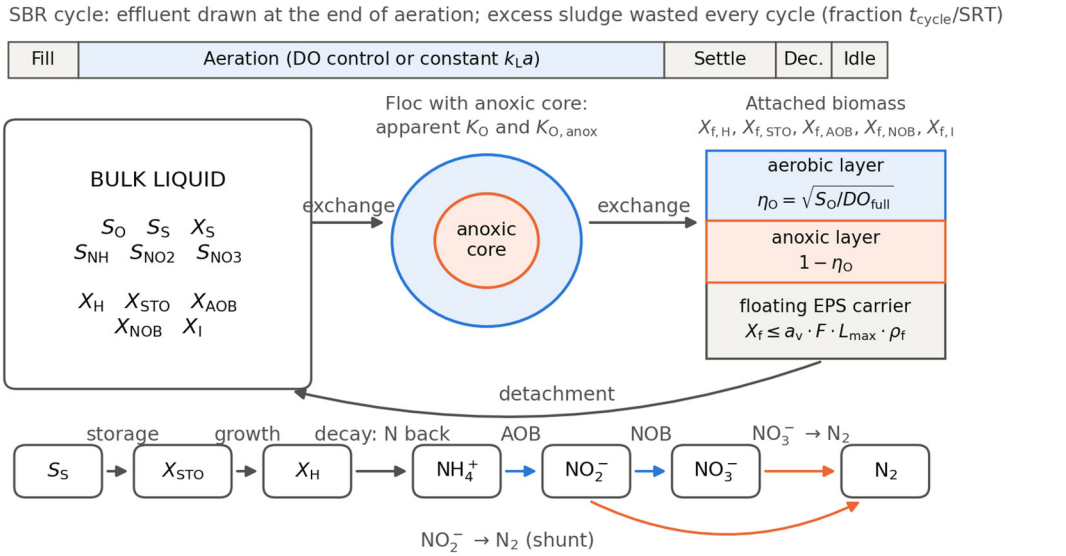

Figure 1. Structure of the model: SBR cycle, suspended flocs with apparent oxygen constants for simultaneous nitrification–denitrification, and attached biomass on floating carriers with an oxygen-penetration-based aerobic fraction; the lower row shows the main nitrogen conversions

the outer layers; measured apparent values rise with floc size (Manser et al., 2005; Wu et al., 2021).

We kept the biofilm module simple on purpose. A full diffusion–reaction description of the film needs parameters that are almost never available for a real plant, and in our experience a lumped description is what an engineer can actually use. The maximum attached inventory is fixed by the geometry of the carriers,

$$X_{f,max} = a_v \cdot F \cdot L_{max} \cdot \rho_f \quad (4)$$

where: a_v is the specific surface area of the carrier (m^2/m^3 of carrier), F the carrier fill fraction, L_{max} the maximum mean biofilm thickness and ρ_f the biomass density in the film.

Attached biomass grows and decays with the same kinetics as the suspended biomass, but only a fraction of the film sees oxygen. For a zero-order oxygen sink the penetration depth grows with the square root of the bulk concentration (Rittmann and McCarty, 2020), so the aerobic fraction was taken as $\eta_O = \min(1, (S_O/DO_{full})^{0.5})$, with DO_{full} the bulk DO at which oxygen would reach the carrier surface. Aerobic processes in the film are scaled by η_O and anoxic processes by $1 - \eta_O$; anoxic processes that need external substrate are further multiplied by $\eta_{sub} = 0.5$ to account for the limited supply of S_S and NOx to the inner layers. Detachment transfers attached biomass to the suspended phase at a rate $k_{det} \cdot (X_f/X_{f,max})^2$, which keeps the film close to, but not above, its geometric capacity. Detached biomass is then subject to normal wasting.

All rates are corrected for temperature with Arrhenius-type coefficients (θ = 1.072 for heterotrophic rates, 1.111 for the maximum growth rates of nitrifiers and 1.116 for their decay), and oxygen saturation is calculated from temperature (Benson and Krause, 1984). The parameter values are listed in Table 1.

SBR operation and numerical solution

The cycle consists of fill, aeration, settling, decanting and idle phases. Filling was treated as instantaneous mixing of the influent with the liquid left from the previous cycle, followed by the unaerated fill period with reactions running. During aeration the DO was either held at a set-point (the aeration term is adjusted so that the oxygen transfer equals the uptake once the set-point is reached, with an upper limit on k_La) or supplied with a constant k_La, depending on how the reactor being simulated was operated. Settling was assumed ideal: the effluent composition equals the soluble composition at the end of aeration, the decanted volume leaves, and all particulate material stays in the reactor. Reactions continue in the retained volume during settling, decanting and idle. At the end of each cycle a fraction t_{cycle}/SRT of the

Table 1. Model parameters at 20 °C

Parameter	Symbol	Value	Unit	Source
Storage rate constant	k_{STO}	5.0	d^{-1}	Gujer et al. (1999)
Maximum heterotrophic growth rate	μ_H	2.0	d^{-1}	Gujer et al. (1999)
Half-saturation, S_S	K_S	2.0	mg COD/L	Gujer et al. (1999)
Half-saturation, storage products	K_{STO}	1.0	g COD/g COD	Gujer et al. (1999)
Maximum storage fraction	$f_{STO,max}$	0.3 or ∞	g COD/g COD	this study
Hydrolysis rate constant / half-saturation	k_H / K_X	3.0 / 1.0	d^{-1} / g COD/g COD	Gujer et al. (1999)
Anoxic reduction factor	η_{NO}	0.6	–	Gujer et al. (1999)
Yield of storage, aerobic / anoxic	$Y_{STO,O2}$ / $Y_{STO,NO}$	0.85 / 0.80	g COD/g COD	Gujer et al. (1999)
Heterotrophic yield, aerobic / anoxic	$Y_{H,O2}$ / $Y_{H,NO}$	0.63 / 0.54	g COD/g COD	Gujer et al. (1999)
Endogenous respiration of X_H, aerobic / anoxic	$b_{H,O2}$ / $b_{H,NO}$	0.2 / 0.1	d^{-1}	Gujer et al. (1999)
Respiration of X_{STO}, aerobic / anoxic	$b_{STO,O2}$ / $b_{STO,NO}$	0.2 / 0.1	d^{-1}	Gujer et al. (1999)
O_2 half-saturation, aerobic heterotrophic processes	K_O	0.2	mg O_2/L	Gujer et al. (1999)
Apparent O_2 inhibition of anoxic processes	$K_{O,anox}$	0.25–1.5	mg O_2/L	calibrated
NOx half-saturation	K_{NOx}	0.5	mg N/L	Gujer et al. (1999)
NH_4 half-saturation for heterotrophic growth	$K_{NH,H}$	0.01	mg N/L	Gujer et al. (1999)
N content of biomass / inert matter	$i_{N,BM}$ / $i_{N,XI}$	0.07 / 0.02	g N/g COD	Gujer et al. (1999)
Inert fraction produced in decay	f_I	0.20	–	Gujer et al. (1999)
Maximum growth rate, AOB / NOB	μ_{AOB} / μ_{NOB}	0.63 / 0.80	d^{-1}	Kobylko (2026)
Half-saturation NH_4 (AOB) / NO_2 (NOB)	$K_{NH,AOB}$ / $K_{NO2,NOB}$	1.2 / 1.2	mg N/L	Kobylko (2026)
Apparent O_2 half-saturation, AOB	$K_{O,AOB}$	2.0–4.0	mg O_2/L	calibrated
O_2 half-saturation, NOB	$K_{O,NOB}$	0.6	mg O_2/L	Kobylko (2026)
Yield AOB / NOB	Y_{AOB} / Y_{NOB}	0.15 / 0.041	g COD/g N	Kobylko (2026)
Decay AOB / NOB (aerobic)	b_{AOB} / b_{NOB}	0.06 / 0.04	d^{-1}	Kobylko (2026)
Factor on μ_{AOB} and μ_{NOB} (sensitivity runs only)	φ	1.0 (0.5, 0.4, 0.3)	–	this study
O_2 level for full film penetration	DO_{full}	4.0	mg O_2/L	assumed
Substrate availability in anoxic film	η_{sub}	0.5	–	assumed
Detachment coefficient	k_{det}	0.1	d^{-1}	assumed
Maximum biofilm thickness / density	L_{max} / ρ_f	250 / 40	µm / kg COD/m³	assumed
Temperature coefficients (μ_H, k_{STO}, b_H; μ_A; b_A)	θ	1.072; 1.111; 1.116	–	Gujer et al. (1999)

suspended solids is wasted; attached biomass is not wasted directly. For continuously fed reactors the same process rates were used in a completely mixed tank with an ideal clarifier.

We integrated the equations with an explicit Euler scheme and a positivity check, with a step of 10–20 s. Halving or doubling the step changed TN removal by less than 0.1%. In a closed batch test (no feed, no aeration, no wasting) total nitrogen was conserved to within 0.001%, and total COD, with oxygen and oxidised nitrogen counted as negative COD, to within 0.003%. Simulations were run until effluent TN and the suspended and attached biomass inventories were stable over eight consecutive cycles; the per-cycle nitrogen balance (N_2 formed + N in wasted sludge + N in effluent = N fed) then closed within 1%. The code was written in Python.

Independent data sets

Two published experiments by other groups were used, chosen because they vary DO or COD/N systematically and report enough operating detail to be simulated (Table 2).

Machat et al. (2019) operated a 32 L hybrid activated sludge reactor with fixed plastic carriers, a settler and sludge recycle, fed continuously with synthetic wastewater (glucose and ammonium sulphate) at an HRT of 27–28 h and an

SRT of 35 d, at 18–26 °C. After a 36-day adaptation, DO was controlled at 0.5–1, 1–2 and about 3 mg/L at C/N 12, and then C/N was reduced to 10, 8 and 4 at DO 1–2 mg/L. Mean TN and ammonium removals for each period are given in the text. The carrier area was not reported, so the reactor was simulated without a biofilm module and the apparent constants were left to absorb the carrier effect. Some details are not stated in the paper and had to be assumed: the DO was taken at the mid-point of each reported range, the adaptation period was assumed to have run at C/N 12 and DO 1.5 mg/L, and the three DO levels were assumed to have lasted about 13 days each, in increasing order.

Ghasemi et al. (2024) ran three aerated moving-bed SBRs of 12.9 L with 40% Kaldnes K3 carriers on a 12-h cycle (0.5 h fill, 8 h aeration, 1.5 h settling, 0.25 h decanting, 1.75 h idle) with a volumetric exchange ratio of 0.5. Synthetic wastewater contained acetate, glucose and sucrose with 60 mg/L ammonium nitrogen, at COD/N 10 and 20. The SRT of the suspended sludge was set to 5, 10 and 15 d by wasting mixed liquor. Air was supplied at a constant rate, so DO was not controlled; ammonium, nitrate and nitrite at the end of aeration and MLSS are reported for all six combinations. Temperature was not given and 25 °C was assumed. The k_La was not fitted to the nitrogen data: it was set to 104.8 d^{-1}, the value at which the simulated DO at the end of aeration in the COD/N 10, SRT 10 d reactor matched the reported 2.5–3.0 mg/L. For the carriers a_v = 500 m^2/m^3 was used; carriers also raise oxygen transfer somewhat (Daigger and Boltz, 2018), which is absorbed in the k_La.

Calibration and testing

Only the two apparent oxygen constants were estimated; all other kinetic and stoichiometric parameters were kept at the values in Table 1. With sparse data, calibrating a few parameters with a clear physical meaning is safer than fitting many (Andraka et al., 2018). For the Machat et al. (2019) data, $K_{O,anox}$ and $K_{O,AOB}$ were varied on a grid (0.5–2.0 and 0.5–4.0 mg/L) and chosen by the root mean square error (RMSE) of TN and ammonium removal in the three DO periods. The C/N series was then simulated with the same values, without any further change, and used as the test. The whole calendar of the experiment was simulated dynamically, because each period lasted about one SRT or less and a steady-state comparison would have been misleading. For the Ghasemi et al. (2024) data, $K_{O,AOB}$ was kept at 2.0 mg/L and $K_{O,anox}$ was selected on the COD/N 10 phase (0.25, 0.5 and 1.0 mg/L were tried); the COD/N 20 phase served as the test. The storage limit $f_{STO,max}$ was not fitted to nitrogen data. Its value, 0.3 g COD/g COD, corresponds to the amount of COD that disappeared almost immediately after feeding in the COD/N 10 reactors (about 265 mg/L), and both the limited and the unlimited ASM3 storage were simulated.

Because the model overestimated nitrification in both data sets (see Results), a common factor φ was applied to the maximum growth rates μ_{AOB} and μ_{NOB} and varied from 1.0 to 0.2, with all other parameters unchanged. φ is not a recalibrated kinetic constant. It stands, in a lumped way, for processes that the model lacks, such as alkalinity limitation, pH inhibition or incomplete adaptation of the nitrifiers, and it was used only to test how sensitive the scenario results are to the rate of nitrification.

Table 2. Independent data sets used for testing

Parameter	Machat et al. (2019)	Ghasemi et al. (2024)
Reactor	Continuous hybrid activated sludge, 32 L, settler and recycle	Aerated moving-bed SBR, 12.9 L (three reactors)
Carrier	Fixed plastic brush, area not reported	Kaldnes K3, 40% of volume
Feed	Synthetic: glucose, $(NH_4)2SO_4$	Synthetic: acetate, glucose, sucrose, $(NH_4)2SO_4$
COD / TN, mg/L	916–933 / 80–232	600 or 1200 / 60
Varied factor	DO 0.5–1, 1–2, ~3 mg/L (C/N 12); C/N 12, 10, 8, 4 (DO 1–2)	COD/N 10 and 20 × SRT 5, 10, 15 d
HRT / SRT / T	27–28 h / 35 d / 18–26 °C	24 h (12-h cycle, exchange 0.5) / 5–15 d / not reported
Aeration	DO controlled	Constant air flow
Data used	TN and NH_4 removal per period	End-of-aeration NH_4, NO_3, NO_2; MLSS
Role in this study	Calibration (DO series), test (C/N series)	Calibration (COD/N 10), test (COD/N 20)

All calibration and test results reported in the Results section refer to φ = 1. The values of φ were selected afterwards using the same ammonium data, so they are not independently validated.

Dairy wastewater scenarios

A generic dairy effluent after fat separation was defined with COD 2000 mg/L (60% readily and 40% slowly biodegradable) and total nitrogen chosen to give COD/N ratios of 10, 15, 20, 30 and 45. Half of the nitrogen was ammonium and half organic, bound to the COD fractions in equal proportion. The SBR had a 12-h cycle (0.5 h fill, 9 h aeration, 1.5 h settling, 0.5 h decanting, 0.5 h idle) and a 25% exchange ratio, which gives an HRT of 48 h and an organic loading rate of 1.0 kg COD/(m³·d). The SRT was 15 d and the temperature 20 °C. DO set-points of 0.5, 1.0, 1.5 and 2.0 mg/L were tested, each with and without floating expanded polystyrene (EPS) carriers (a_v = 550 m²/m³, F = 0.30, L_{max} = 250 µm). The apparent constant from the Machat et al. (2019) calibration was used as the base case, $K_{O,anox}$ = 1.5 mg/L, with $K_{O,AOB}$ = 2.0 mg/L because the data did not constrain it, and the runs were repeated with $K_{O,anox}$ = 0.5 and 1.0 mg/L to see how much the conclusions depend on it. Nitrogen fed in each cycle was split into three outputs: N_2 formed by denitrification, nitrogen in the wasted sludge and nitrogen in the effluent.

The assumed composition was compared with literature and operational data for dairy plants (Table 3). A COD of 2000 mg/L is close to the mean COD of the influent to the Michów treatment plant, which receives dairy effluent together with 18–25% of domestic sewage (1808 mg/L; Zawadzka et al., 2021). It also lies within the range of the pre-treated effluent of the Ciechanów dairy (374–2874 mg/L; Gugała et al., 2015) and of mixed dairy effluents in general (Kolev Slavov, 2017). The ratio of mean COD to mean TN was 23 at Michów, 35 for the pre-treated and 49–52 for the raw Ciechanów effluent. The real effluents therefore fall in the middle and upper part of the scenario range. The lower end, COD/N 10–15, is lower than at these plants; it stands for nitrogen-rich effluents, for example dairy wastewater after anaerobic pretreatment, which removes much of the COD but little of the nitrogen. Both plants reported a BOD_5/COD ratio of 0.58–0.59, whereas the scenario COD was taken as fully biodegradable. If 10–20% of the COD of a real effluent is not biodegradable, the scenario with a given COD/N corresponds to a raw effluent with a COD/N about 10–25% higher. This assumption affects the predicted biomass production and hence the share of nitrogen in the sludge. For a raw effluent with COD/N 20 and 20% non-biodegradable COD, for example, the sludge share would be close to that of a COD/N 16 scenario, about 20% instead of 26%. The sensitivity analysis with φ concerns nitrification and does not cover this uncertainty in COD fractionation. The comparison in Table 3 therefore supports the plausibility of the assumed ranges, not the exact composition of the effluent of a particular plant.

RESULTS AND DISCUSSION

Behaviour of the continuous hybrid reactor

The goodness-of-fit statistics for the two independent data sets are given in Table 4. The results of each comparison are discussed separately below.

The fit on the DO series gave $K_{O,anox}$ = 1.5 mg/L and $K_{O,AOB}$ = 4.0 mg/L. The second constant, however, was not clearly identified: when its value was changed from 0.5 to 4 mg/L, the calibration RMSE changed by less than 0.5 percentage points. The overall calibration RMSE was 17.2 percentage points, and almost all of this error came from the low-DO period discussed below.

With these parameter values the model correctly reproduced the decline of TN removal at high DO: the simulated value was 71.4% against 72% in the experiment at DO ≈ 3 mg/L. Under these conditions the anoxic zone inside the flocs shrinks, and nitrate starts to accumulate as a result (Figure 2a). The model could not, however, reproduce the behaviour of the system at low DO. At DO 0.5–1 mg/L the experiment showed incomplete nitrification: ammonium removal was 73.7% and its effluent concentration 19.7 mg/L NH_4-N. In the model, by contrast, nitrification was almost complete and TN removal reached about 98%. Nor could it reproduce the optimum DO range of 1–2 mg/L measured in the experiment: in the model the treatment efficiency kept increasing as the oxygen concentration decreased.

The series of experiments at different C/N ratios was a more objective test of the model, since none of these results had been used to tune it. This test, however, turned out to be harder than expected. At C/N 10 and 8 the model gave TN

Table 3. Composition of the scenario effluent compared with literature and operational data for dairy plants (COD/N is the ratio of the mean values)

Source	Type of data	COD, mg/L	TN, mg/L	NH_4-N, % of TN	COD/N
Kolev Slavov (2017)	Review, mixed dairy effluents	500–10 400	10–660	–	–
Zawadzka et al. (2021), Michów WWTP, Poland	Influent: dairy effluent with 18–25% of domestic sewage; mean (range), n = 29, 2017–2021	1808 (158–3807)	78.5 (24.1–95.4)	34	23
Gugała et al. (2015), Ciechanów dairy, Poland	Raw total effluent, morning and afternoon samples	3900–5890	79–114	–	49–52
	Effluent after neutralisation and fat separation; mean (range) over one year	1388 (374–2874)	40 (13–75)	–	35
This study	Scenarios	2000	44–200	50	10–45

Table 4. Goodness of fit against the independent data sets

Data set	Series	Role	Measure	Model, ASM3 storage	Model, storage limit 0.3
Machat et al. (2019)	DO 0.5–1, 1–2, ~3 mg/L	Calibration	RMSE of TN and NH_4 removal, percentage points	17.2	17.2
	C/N 10 and 8	Test	RMSE of TN and NH_4 removal, percentage points	5.7	5.7
	C/N 4	Test	Error of TN / NH_4 removal, percentage points	−16.6 / +17.8	−16.6 / +17.8
Ghasemi et al. (2024)	COD/N 10, SRT 5–15 d	Calibration	RMSE of NH_4 and NO_3, mg N/L	10.8	11.6
			Error of MLSS, %	−12 to −3	−24 to −4
	COD/N 20, SRT 5–15 d	Test	RMSE of NH_4 and NO_3, mg N/L	8.2	10.0
			Error of MLSS, %	+88 to +146	−19 to +39

removal of 83.2% and 67.4%, whereas 86.1% and 77.0%, respectively, were obtained in the experiment. The RMSE for TN and ammonium removal in these two regimes was 5.7 percentage points (Figure 2b). The model thus correctly reproduced both the direction and the approximate size of the decrease in efficiency as C/N decreased.

This agrees with the expected behaviour of the process: as the amount of organic carbon per unit of nitrogen decreases, denitrification becomes increasingly limited by the availability of organic substrate, so part of the nitrate remains in the treated water. A similar dependence has been described for moving-bed systems and SBRs over a wide range of C/N ratios (Iannacone et al., 2019; Tao and Chang, 2025).

At C/N 4 the agreement was much worse. The simulated TN removal was 36% against 53% in the experiment, and nitrification in the model was almost complete, whereas in reality its efficiency was only 82%. In all six regimes studied the model also overestimated ammonium removal (Figure 2c).

Two features of the experiment probably contributed to this discrepancy. In our view, alkalinity may have been the most important. Nitrification of 230 mg/L ammonium at C/N 4 requires about 1.6 g/L of alkalinity as $CaCO_3$. This is far more than synthetic wastewater without additional buffering usually contains. The pH in the reactor also varied between 6 and 8. The model does not include an alkalinity balance or inhibition of nitrification by low pH. In addition, during the low-DO period the nitrifier population had developed at a lower nitrogen load, because the load was increased gradually during adaptation. The experimental period itself was shorter than half the sludge age. The published data do not make it possible to establish which of these factors had the greater effect. The explanations given here are possible causes of the discrepancy, not corrections introduced into the model.

Behaviour of the aerated moving-bed SBR

Figure 3 compares the concentrations at the end of aeration and the MLSS values for the six reactors studied by Ghasemi et al. (2024). The best fit for the COD/N 10 regime was obtained with the lowest $K_{O,anox}$ tested, 0.25 mg/L, which is close to the standard ASM3 value. This result

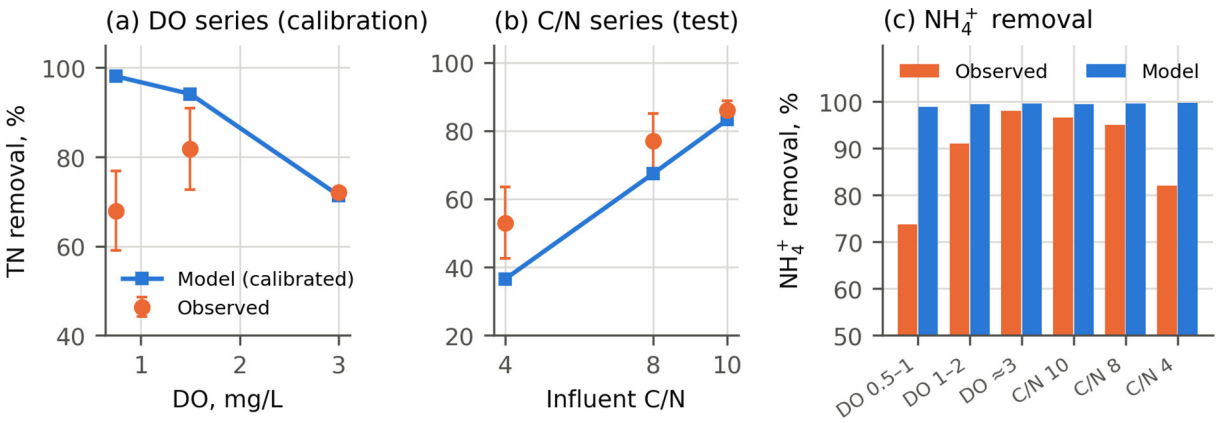

Figure 2. Comparison with the continuous hybrid reactor of Machat et al. (2019): (a) TN removal in the DO series used for calibration; (b) TN removal in the C/N series predicted without further adjustment; (c) ammonium removal in all periods. Error bars show the standard deviations reported by the authors

is logical: after the first hour of operation the DO in these reactors rose to 2.5–4 mg/L, and at such levels intensive SND inside the flocs is unlikely.

At COD/N 10 the simulated MLSS was 3–12% lower than the experimental values for all three sludge ages. This shows that the model describes the growth and decay of biomass and its removal from the reactor realistically enough. These processes determine the total sludge mass and, accordingly, the amount of nitrogen that can be removed with the biomass.

The model reproduced the nitrate concentration at the end of aeration satisfactorily: the simulated values were 6.6–11.0 mg/L against 9.0–11.1 mg/L in the experiment. For ammonium the agreement was much worse. After 8 h of aeration, 10–18 mg/L NH_4-N remained in the experimental reactors, whereas the model predicted almost complete nitrification. Changing $K_{O,anox}$ or the temperature within 12–25 °C had practically no effect on this result: the RMSE for ammonium and nitrate remained within 9–12 mg/L. The persistently elevated ammonium concentration is most likely related to a process not included in the model, rather than to an unfortunate choice of the two apparent oxygen constants. Insufficient alkalinity may again be one of the most likely causes. The published work gives no information on adding a buffer to the synthetic wastewater.

The results for COD/N 20 revealed a different problem with the model. With unlimited storage, as in the basic ASM3 concept, practically all the added COD was converted into storage products and then consumed. As a result, the sludge concentration was overestimated by a factor of 1.9–2.5, and because of the high oxygen consumption the system remained without sufficient DO for a large part of the aeration period. The nitrate concentration stayed close to zero.

In the experiment the MLSS was much lower, and part of the COD remained in the treated water (38–190 mg/L). After the storage limit was introduced, the simulated MLSS at sludge ages of 10 and 15 d came closer to the experimental values: 2.2 and 3.4 g/L against 1.6 and 2.9 g/L, respectively. Even so, 350–450 mg/L of soluble COD remained in the model, several times more than in the experiment. The ammonium concentration also remained overestimated.

The authors of the experiment note that 88–90% of the COD disappeared within the first minutes after feeding, while DO did not fall to zero. Such rapid uptake of organic matter without a corresponding oxygen demand may indicate anaerobic storage of carbohydrates during filling, for example as glycogen. This mechanism is not included in ASM3. In short, this data set characterises well the model's ability to reproduce sludge production at a moderate COD/N ratio, but it does not provide sufficient grounds for assessing the nitrification kinetics.

Both independent comparisons show that the model generally describes denitrification limited by the availability of organic carbon, as well as activated sludge production at COD/N around 8–10, adequately. In both experiments, however, nitrification was slower than the literature kinetics adopted in the model predict. The scenario results below have to be read with this limitation in mind. Where a result depends directly on the

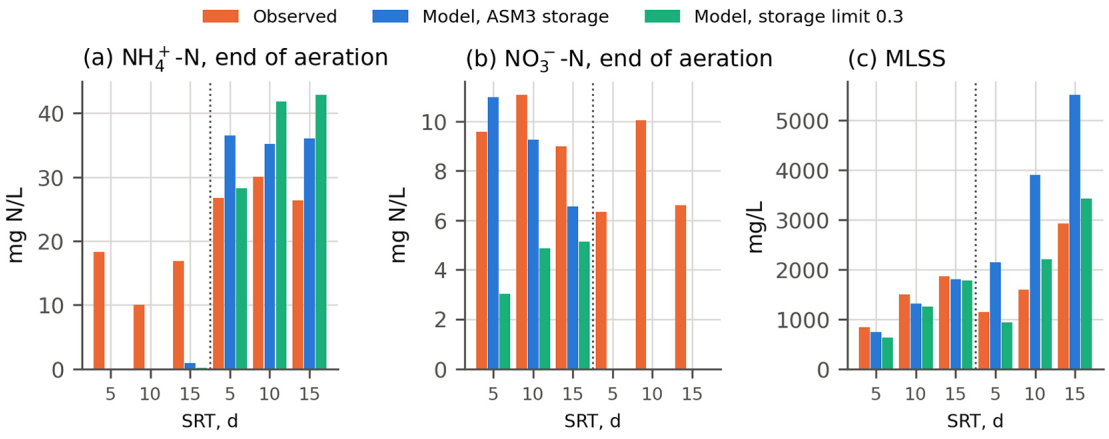

Figure 3. Comparison with the aerated moving-bed SBRs of Ghasemi et al. (2024): (a) ammonium and (b) nitrate at the end of aeration, (c) MLSS, for COD/N 10 and 20 and SRT 5, 10 and 15 d; the model is shown with the original ASM3 storage and with the storage limit $f_{STO,max} = 0.3$

assumption of complete nitrification, the model probably gives an overestimate. How much this matters for the scenario results is examined below with reduced nitrifier growth rates.

Nitrogen pathways in the dairy wastewater scenarios

Figure 4 shows the distribution of the nitrogen entering the SBR at DO 1.0 mg/L. At COD/N 10 about 88% of the nitrogen was converted to N_2, while 12% was removed with the excess sludge. As the COD/N ratio increased, the share of nitrogen passing into biomass grew gradually: to 26% at COD/N 20 and to 58% at COD/N 45. Accordingly, the share of nitrogen converted to N_2 fell to 42%. In all the scenarios considered, the share of nitrogen remaining in the treated water was below 0.2%. This is because at an HRT of 48 h and an aeration time of 9 h nitrification and denitrification in the model were practically complete. The nitrogen balance closed to within 1% in every scenario.

The reason for this redistribution of nitrogen is fairly simple. At a given sludge age, biomass growth per unit of COD removed remains approximately constant. As the COD load increases, so does the amount of nitrogen needed to form new biomass. At a high COD/N ratio, much of the nitrogen entering the reactor is first used for microbial growth, and only the remainder can be nitrified and denitrified. This behaviour agrees with the well-known approximate nutrient ratio for activated sludge of BOD_5:N ≈ 100:5 (Metcalf & Eddy, Inc. et al., 2014).

At COD/N above about 50 the model showed signs of growth limitation by nitrogen deficiency, which reduces the completeness of COD removal. In practice, nitrogen compounds may be added to the wastewater under such conditions to prevent deterioration of sludge properties and bulking (Guo et al., 2014). This range was not considered further.

From a practical point of view, this means that for dairy wastewater with COD/N above about 20 even very high TN removal does not necessarily indicate high SND efficiency. For example, at COD/N 45 more than half of the nitrogen can be removed with the excess sludge even without significant denitrification. When different reactor operating regimes are compared or the effect of carriers is assessed, it is advisable to determine, at least approximately, the amount of nitrogen leaving with the excess sludge. This can be estimated from biomass growth and its nitrogen content.

Overall, the use of carriers had little effect on total TN removal as long as nitrification proceeded at the literature rates. They did, however, somewhat change the route of nitrogen removal, above all the ratio between its conversion to N_2 and its accumulation in biomass. With expanded polystyrene carriers, the share of nitrogen converted to N_2 at DO 1.0 mg/L was 0.7 percentage points higher at COD/N 10 and 4.8 points higher at COD/N 45. At other DO values the difference reached 7.8 points. The share of nitrogen removed with the sludge decreased accordingly. This is explained by the fact that the biomass attached to the carriers is not removed with the

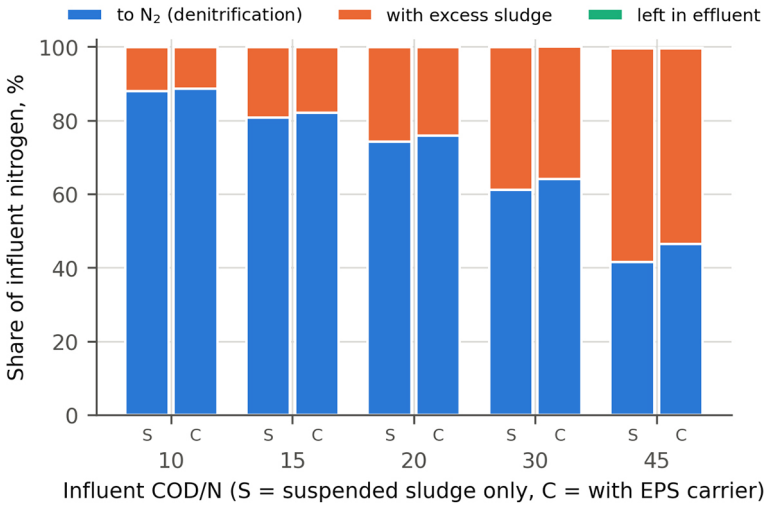

Figure 4. Fate of influent nitrogen in SBR scenarios for dairy wastewater at DO 1.0 mg/L: conversion to N_2, removal with excess sludge and residual in the effluent, without (S) and with (C) floating EPS carriers

excess activated sludge. So, at the same age of the suspended sludge, less new biomass leaves the reactor, and with it less bound nitrogen.

This result agrees with the data of Sirianuntapiboon et al. (2005), who obtained about three times less excess sludge for dairy wastewater in an SBR with plastic carriers than in a similar reactor without carriers. Respirometric studies of hybrid systems also indicate differences in activity between attached and suspended biomass (Piechna and Żubrowska-Sudoł, 2017). The effect of carriers is thus related not only to an increase in the total amount of biomass, but also to a change in its distribution between the attached and suspended fractions.

Influence of DO and of the apparent oxygen constant

The effect of the DO set-point and its interaction with $K_{O,anox}$ are shown in Figure 5. At COD/N 10 the DO concentration had a noticeable effect on treatment efficiency. With the base value of the constant, TN removal decreased from almost 100% at DO 0.5–1.0 mg/L to 93.6% at DO 2.0 mg/L. It was precisely at this DO increase that nitrate started to accumulate in the system. With $K_{O,anox}$ = 0.5 mg/L the decrease in efficiency was even more pronounced: at DO 2.0 mg/L TN removal was 85.3%.

For COD/N 20 and 45 TN removal remained above 95% over the whole DO range studied and depended little on $K_{O,anox}$. This is because the amount of available stored substrate was sufficient to reduce all the nitrate formed during nitrification. As the DO concentration in the water increases, oxygen also penetrates deeper into the biofilm (Cao et al., 2017). In the model this effect is taken into account in a simplified way, through the aerobic fraction of the biofilm η_O, which grows with DO and correspondingly reduces the anoxic part of the film.

Unlike total TN removal, the ratio between nitrogen converted to N_2 and nitrogen removed with the sludge depended much more on COD/N than on DO or $K_{O,anox}$. At all DO values and $K_{O,anox}$ values studied, the share of nitrogen in the excess sludge was 11–14% at COD/N 10, 24–28% at COD/N 20 and 55–64% at COD/N 45. For the last range the change in DO played the larger role.

The results obtained make it possible to separate the conclusions that are sufficiently robust from those that require careful interpretation. The distribution of nitrogen between N_2 and the excess sludge is determined mainly by process stoichiometry and sludge age, and it proved to be insensitive to the uncertain SND parameters. In contrast, the overall TN removal efficiency at low COD/N, especially in the DO range where it starts to decrease, depends more on these parameters and on the rate of nitrification.

Since in both independent experiments nitrification was slower than the model predicts, the results for this process should be treated with caution. Still, the calculations show that maintaining DO at about 1 mg/L for wastewater with COD/N around 10 is a justified regime within the adopted model assumptions. At this DO value the risk of

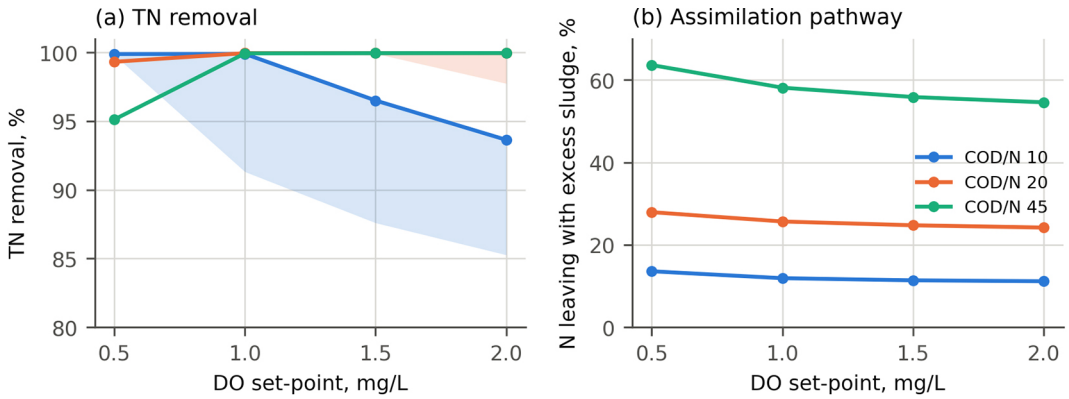

Figure 5. Effect of the DO set-point on (a) TN removal and (b) the share of nitrogen leaving with the excess sludge at COD/N 10, 20 and 45 (reactor without carriers); lines show the base case ($K_{O,anox}$ = 1.5 mg/L), shaded bands the range for $K_{O,anox}$ = 0.5–1.5 mg/L

nitrate accumulation is small and the need for excess aeration is reduced. With slower nitrification, however, this holds only for the reactor with carriers, as shown below.

The cycle profile for COD/N 20 with carriers (Figure 6) shows that soluble COD was exhausted about 3.2 h after the start of aeration and ammonium after about 3.9 h. The nitrite and nitrate concentrations remained below 0.25 mg/L throughout the cycle. Under these model conditions, more than half of the 9-h aeration phase had practically no effect on further nitrogen removal. In theory, shortening the aeration time or switching to intermittent aeration after nitrification is complete could reduce energy consumption. This possibility, however, must be verified experimentally, taking into account that in real systems nitrification may proceed more slowly than the model predicts. With φ = 0.5 the ammonium was not exhausted within the 9-h aeration phase (5.9 mg/L remained at its end), so this reserve exists only if nitrification proceeds at the assumed rate.

Effect of slower nitrification on the nitrogen pathways

Both independent data sets showed slower nitrification than the model, so the scenarios were repeated with reduced nitrifier growth rates. With φ = 0.5 the simulated residual ammonium at the end of aeration in the COD/N 10 reactors of Ghasemi et al. (2024) came close to the measured values: the RMSE for ammonium fell from 15.4 to 5.5 mg/L, with 12–25 mg/L simulated against 10–18 mg/L measured. For the reactor of Machat et al. (2019) the closest match was obtained with φ = 0.4. The RMSE for ammonium removal in all six periods fell from 13.2 to 6.7 percentage points, and the simulated ammonium removal at DO 0.5–1 mg/L was 76% against 73.7% measured. At φ = 0.3 the model underestimated nitrification in both cases. Because φ was chosen using these ammonium data, this agreement is not an independent validation of the modified model; it only indicates the range of nitrification rates for which the scenarios should be tested. The scenarios were therefore repeated with φ = 0.5 and 0.4, and with φ = 0.3 as a stress test (Table 5).

The share of nitrogen leaving with the excess sludge proved insensitive to φ. Across all COD/N ratios, DO set-points and both reactor types it changed by at most 2.2 percentage points. The amount of nitrogen incorporated into biomass depends on heterotrophic growth on the COD, not on the rate at which the remaining ammonium is oxidised. The assumed 50:50 split between ammonium and organic nitrogen did not matter either: with 30% ammonium, close to the 34% at Michów (Table 3), the shares changed by less than 1 percentage point.

What did change was the fate of the nitrogen not taken up by the biomass. With φ = 0.5 and DO 0.5–1.0 mg/L, the nitrifiers were washed out of the suspended-growth SBR at the SRT of 15 d. Most of the remaining nitrogen then left with the effluent as ammonium, and TN removal fell to 14–64% (20–62% at DO 1.0 mg/L), practically equal to the share bound in the sludge. At COD/N 45 the reactor thus still removed about 60% of TN with almost no nitrification, which illustrates once more why TN removal alone says little about denitrification. With carriers, nitrifiers retained in the biofilm kept nitrification going at DO 1.0 mg/L, though not at 0.5 mg/L, and TN removal was 86–99.6%.

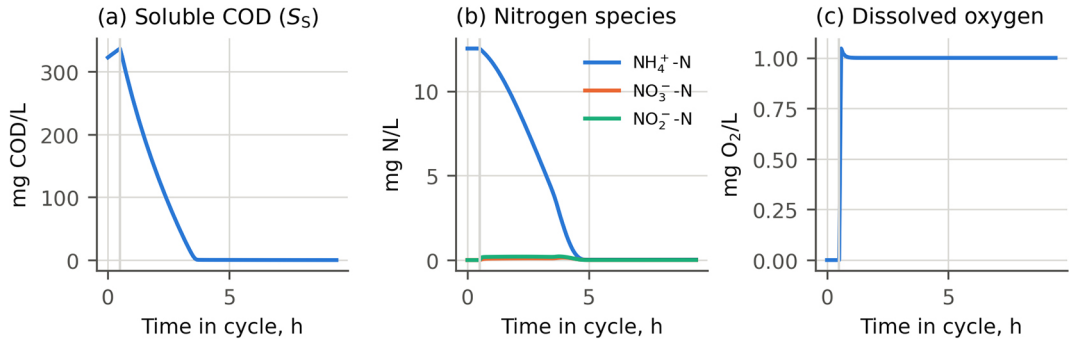

Figure 6. Simulated course of (a) soluble COD, (b) nitrogen species and (c) dissolved oxygen during one cycle at COD/N 20 and DO 1.0 mg/L with EPS carriers; the vertical line marks the end of filling

Table 5. Fate of influent nitrogen at DO 1.0 mg/L with the literature (φ = 1) and reduced (φ = 0.5 and 0.4) nitrifier growth rates: N_2 / excess sludge / effluent, % of nitrogen fed; S – without carriers, C – with EPS carriers

COD/N	φ = 1, S	φ = 1, C	φ = 0.5, S	φ = 0.5, C	φ = 0.4, S	φ = 0.4, C
10	88 / 12 / 0	89 / 11 / 0	7 / 13 / 80	88 / 12 / 0	0 / 13 / 87	25 / 12 / 63
20	74 / 26 / 0	76 / 24 / 0	9 / 26 / 65	70 / 24 / 6	0 / 26 / 73	19 / 25 / 56
30	61 / 39 / 0	64 / 36 / 0	7 / 39 / 54	53 / 37 / 11	0 / 39 / 60	15 / 37 / 48
45	42 / 58 / 0	46 / 53 / 0	3 / 59 / 38	31 / 55 / 14	0 / 59 / 41	9 / 55 / 35

At DO 1.5–2.0 mg/L both reactor types removed 90–99.9% of TN. With φ = 0.4 the reactor with carriers needed DO 1.5–2.0 mg/L (TN removal 81–99.8%), while the suspended-growth reactor did not nitrify fully even at 2.0 mg/L (61–74%).

The overestimation of nitrification therefore does not substantially affect the predicted share of influent nitrogen removed with the excess sludge. However, it strongly affects the partitioning of the remaining nitrogen between N_2 production and discharge with the effluent, and with it overall TN removal, the appropriate DO set-point and the role of the carriers. At COD/N 45 without carriers, for example, the share of nitrogen converted to N_2 at DO 1.0 mg/L fell from 42% to 3% at φ = 0.5, while the share in the sludge changed only from 58% to 59% (Table 5). If nitrification at a real plant is as slow as in the two experiments, a DO of about 1 mg/L is sufficient only with carriers, and the carriers matter not for denitrification but for keeping the nitrifiers in the reactor. This is the classical argument for hybrid systems: slow-growing nitrifiers are retained independently of sludge wasting (Ødegaard, 2006).

Limitations

The model describes the reactor as a completely mixed system and represents the biofilm in lumped form. The parameters characterising the detailed structure of the biofilm (DO_{full}, η_{sub}, detachment) were not calibrated, because the published data sets did not contain enough information to determine them. In one of the studies the total carrier surface area was unknown, and in the other the attached biomass was measured only as the mass per carrier element.

The model also does not include an alkalinity balance, the effect of pH, anaerobic storage of carbohydrates or N_2O formation.

The most important limitation, however, concerns the data used for testing. Both independent data sets were obtained in laboratory or pilot reactors of 12.9 and 32 L fed with synthetic wastewater made of glucose, acetate, sucrose and ammonium sulphate. Real dairy effluent differs from such feeds in ways that matter for the nitrogen pathways. Most of its nitrogen is organic and has to be ammonified first, part of the COD enters the reactor as fats and proteins, and its composition and pH change over the working day (Kolev Slavov, 2017). The agreement reported here should therefore be regarded as a preliminary validation. Before the model is used for design, it has to be confirmed with data from pilot or full-scale plants treating real dairy wastewater. Such data should preferably include the production of excess sludge and its nitrogen content, so that the

nitrogen balance can be closed directly. The scenario calculations, in turn, were performed for an assumed composition, which was compared with data from dairy plants (Table 3) but not with measurements at a specific plant.

Even so, the comparison with independent experimental data is an important part of this work. It makes it possible to assess which conclusions of the model hold when tested against data that were not used to build it, and which results require careful interpretation or further improvement of the model.

CONCLUSIONS

1. The developed model based on ASM3, with two-step nitrification, limited substrate storage, apparent oxygen constants and a lumped biofilm whose amount is limited by the available carrier surface, closes the nitrogen and COD balances to within 0.003%. Halving or doubling the integration time step changed TN removal by less than 0.1%.
2. After only two apparent oxygen constants were calibrated at different DO levels, the model adequately reproduced total nitrogen and ammonium removal in the C/N range 8–10 without further calibration, with an RMSE of 5.7 percentage points. For the aerated moving-bed SBR the model also reproduced the activated sludge concentration (MLSS) and the end-of-cycle nitrate at COD/N 10 well. In both cases, however, the model overestimated the intensity of nitrification. Both data sets were obtained with synthetic wastewater, so this validation is preliminary and has to be confirmed with data from plants treating real dairy wastewater.
3. According to the scenario simulations for dairy wastewater (COD 2000 mg/L, sludge age 15 d), the share of nitrogen removed with the excess activated sludge increases from about 12% at COD/N 10 to 58% at COD/N 45. Changes in the dissolved oxygen concentration and in the value of the apparent oxygen constant had practically no effect on this nitrogen distribution. Nor did slower nitrification: when the nitrifier growth rates were multiplied by 0.4–0.5 to approach the residual ammonium measured in both experiments, the share of nitrogen in the sludge changed by at most 2.2 percentage points, although the share converted to N_2 decreased and the share discharged with the effluent increased.
4. The use of floating expanded polystyrene carriers practically did not change overall TN removal with the literature nitrification kinetics. At the same time, at COD/N 30–45 the share of nitrogen converted to N_2 increased by 3–8 percentage points, depending on the DO concentration. This is because the biomass attached to the carriers is not removed with the excess activated sludge. With nitrification as slow as in the two experiments, however, the carriers were decisive: at DO 1.0 mg/L they kept TN removal at 86–99.6%, whereas the suspended-growth reactor lost its nitrifiers and removed only 20–62% of TN.
5. At COD/N 45 more than half of the nitrogen removed from the liquid phase is incorporated into the excess activated sludge. For dairy wastewater with a high content of organic matter, therefore, a high TN removal on its own does not allow the actual efficiency of denitrification to be assessed. A noticeable decrease in TN removal with increasing DO was observed only at the lowest COD/N ratio studied, close to 10, when the DO set-point exceeded about 1 mg/L, provided that nitrification proceeds at the literature rates.

Acknowledgements

The author thanks the staff of the Department of Water Supply, Water Disposal and Drilling Engineering of the National University of Water and Environmental Engineering and personally Prof. Viktor Kovalchuk for their support.

REFERENCES

1. Ahmad, T., Aadil, R. M., Ahmed, H., Rahman, U. U., Soares, B. C. V., Souza, S. L. Q., Pimentel, T. C., Scudino, H., Guimarães, J. T., Esmerino, E. A., Freitas, M. Q., Almada, R. B., Vendramel, S. M. R., Silva, M. C., Cruz, A. G. (2019). Treatment and utilization of dairy industrial waste: A review. *Trends in Food Science & Technology*, *88*, 361–372. https://doi.org/10.1016/j.tifs.2019.04.003
2. Andraka, D., Piszczatowska, I., Dawidowicz, J., Kruszyński, W. (2018). Calibration of activated sludge model with scarce data sets. *Journal of Ecological Engineering*, *19*(6), 182–190. https://doi.org/10.12911/22998993/93793
3. Arnaldos, M., Amerlinck, Y., Rehman, U., Maere, T., Van Hoey, S., Naessens, W., Nopens, I. (2015). From the affinity constant to the half-saturation

index: Understanding conventional modeling concepts in novel wastewater treatment processes. *Water Research*, *70*, 458–470. https://doi.org/10.1016/j.watres.2014.11.046

4. Benson, B. B., Krause, D. (1984). The concentration and isotopic fractionation of oxygen dissolved in freshwater and seawater in equilibrium with the atmosphere. *Limnology and Oceanography*, *29*(3), 620–632. https://doi.org/10.4319/lo.1984.29.3.0620
5. Boltz, J. P., Johnson, B. R., Daigger, G. T., Sandino, J. (2009). Modeling integrated fixed-film activated sludge and moving-bed biofilm reactor systems I: Mathematical treatment and model development. *Water Environment Research*, *81*(6), 555–575. https://doi.org/10.2175/106143008x357066
6. Cao, Y., Zhang, C., Rong, H., Zheng, G., Zhao, L. (2017). The effect of dissolved oxygen concentration (DO) on oxygen diffusion and bacterial community structure in moving bed sequencing batch reactor (MBSBR). *Water Research*, *108*, 86–94. https://doi.org/10.1016/j.watres.2016.10.063
7. Cruz Bournazou, M. N., Arellano-Garcia, H., Wozny, G., Lyberatos, G., Kravaris, C. (2012). ASM3 extended for two-step nitrification–denitrification: A model reduction for sequencing batch reactors. *Journal of Chemical Technology & Biotechnology*, *87*(7), 887–896. https://doi.org/10.1002/jctb.3694
8. Daigger, G. T., Boltz, J. P. (2018). Oxygen transfer in moving bed biofilm reactor and integrated fixed film activated sludge processes. *Water Environment Research*, *90*(7), 615–622. https://doi.org/10.2175/106143017x15054988926596
9. Ghasemi, M., Hasani Zonoozi, M., Hoseini Shamsabadi, M. J. (2024). Simultaneous nitrification and denitrification pattern in aerated moving-bed sequencing batch reactor: Choosing appropriate SRT for different COD/N ratios. *Water Practice & Technology*, *19*(5), 1920–1935. https://doi.org/10.2166/wpt.2024.124
10. Gugała, M., Zarzecka, K., Sikorska, A. (2015). Wastewater management in food processing enterprises – a case study of the Ciechanów Dairy Cooperative. *Journal of Ecological Engineering*, *16*(1), 178–183. https://doi.org/10.12911/22998993/605
11. Gujer, W., Henze, M., Mino, T., van Loosdrecht, M. (1999). Activated Sludge Model No. 3. *Water Science and Technology*, *39*(1), 183–193. https://doi.org/10.2166/wst.1999.0039
12. Guo, J., Peng, Y., Wang, S., Yang, X., Yuan, Z. (2014). Filamentous and non-filamentous bulking of activated sludge encountered under nutrients limitation or deficiency conditions. *Chemical Engineering Journal*, *255*, 453–461. https://doi.org/10.1016/j.cej.2014.06.075
13. Henze, M., Gujer, W., Mino, T., van Loosdrecht, M. (2015). *Activated sludge models ASM1, ASM2, ASM2d and ASM3*. IWA Publishing. https://doi.org/10.2166/9781780402369 (Original work published 2000)
14. Hiatt, W. C., Grady, C. P. L. (2008). An updated process model for carbon oxidation, nitrification, and denitrification. *Water Environment Research*, *80*(11), 2145–2156. https://doi.org/10.2175/106143008x304776
15. Iacopozzi, I., Innocenti, V., Marsili-Libelli, S., Giusti, E. (2007). A modified Activated Sludge Model No. 3 (ASM3) with two-step nitrification–denitrification. *Environmental Modelling & Software*, *22*(6), 847–861. https://doi.org/10.1016/j.envsoft.2006.05.009
16. Iannacone, F., Di Capua, F., Granata, F., Gargano, R., Pirozzi, F., Esposito, G. (2019). Effect of carbon-to-nitrogen ratio on simultaneous nitrification denitrification and phosphorus removal in a microaerobic moving bed biofilm reactor. *Journal of Environmental Management*, *250*, 109518. https://doi.org/10.1016/j.jenvman.2019.109518
17. IWA Task Group on Biofilm Modeling. (2015). *Mathematical modeling of biofilms*. IWA Publishing. https://doi.org/10.2166/9781780402482 (Original work published 2006)
18. Jin, Y., Ding, J., Zhan, W., Du, J., Wang, G., Pang, J., Ren, N., Yang, S. (2023). Effect of dissolved oxygen concentration on performance and mechanism of simultaneous nitrification and denitrification in integrated fixed-film activated sludge sequencing batch reactors. *Bioresource Technology*, *387*, 129616. https://doi.org/10.1016/j.biortech.2023.129616
19. Kaelin, D., Manser, R., Rieger, L., Eugster, J., Rottermann, K., Siegrist, H. (2009). Extension of ASM3 for two-step nitrification and denitrification and its calibration and validation with batch tests and pilot scale data. *Water Research*, *43*(6), 1680–1692. https://doi.org/10.1016/j.watres.2008.12.039
20. Keene, N. A., Reusser, S. R., Scarborough, M. J., Grooms, A. L., Seib, M., Santo Domingo, J., Noguera, D. R. (2017). Pilot plant demonstration of stable and efficient high rate biological nutrient removal with low dissolved oxygen conditions. *Water Research*, *121*, 72–85. https://doi.org/10.1016/j.watres.2017.05.029
21. Kobylko, I. (2026). Mathematical model of simultaneous nitrification-denitrification in a sequencing batch reactor with floating biofilm carriers: Software implementation and parametric sensitivity analysis (in Ukrainian). *Proceedings of the NTUU "Igor Sikorsky KPI". Series: Chemical Engineering, Ecology and Resource Saving*, (2), 45–52. https://doi.org/10.20535/2617-9741.2.2026.365627
22. Kolev Slavov, A. (2017). Dairy wastewaters – general characteristics and treatment possibilities – A review. *Food Technology and Biotechnology*, *55*(1), 14–28. https://doi.org/10.17113/ftb.55.01.17.4520

23. Layer, M., Villodres, M. G., Hernandez, A., Reynaert, E., Morgenroth, E., Derlon, N. (2020). Limited simultaneous nitrification-denitrification (SND) in aerobic granular sludge systems treating municipal wastewater: Mechanisms and practical implications. *Water Research X*, *7*, 100048. https://doi.org/10.1016/j.wroa.2020.100048
24. Li, W., Li, Y. J., Lee, S. M.-Y., Mok, K. M., Hao, T. (2019). Nitrogen removal in moving bed sequencing batch reactors with polyurethane foam cube and luffa sponge carrier materials. *Journal of Environmental Engineering*, *145*(6), 04019025. https://doi.org/10.1061/(asce)ee.1943-7870.0001534
25. Machat, H., Boudokhane, C., Roche, N., Dhaouadi, H. (2019). Effects of C/N ratio and DO concentration on carbon and nitrogen removals in a hybrid biological reactor. *Biochemical Engineering Journal*, *151*, 107313. https://doi.org/10.1016/j.bej.2019.107313
26. Makinia, J., Rosenwinkel, K.-H., Phan, L.-C. (2006). Modification of ASM3 for the determination of biomass adsorption/storage capacity in bulking sludge control. *Water Science and Technology*, *53*(3), 91–99. https://doi.org/10.2166/wst.2006.079
27. Manser, R., Gujer, W., Siegrist, H. (2005). Consequences of mass transfer effects on the kinetics of nitrifiers. *Water Research*, *39*(19), 4633–4642. https://doi.org/10.1016/j.watres.2005.09.020
28. Metcalf & Eddy, Inc., Tchobanoglous, G., Stensel, H. D., Tsuchihashi, R., Burton, F. (2014). *Wastewater engineering: Treatment and resource recovery* (5th ed.). McGraw-Hill Education.
29. Ødegaard, H. (2006). Innovations in wastewater treatment: The moving bed biofilm process. *Water Science and Technology*, *53*(9), 17–33. https://doi.org/10.2166/wst.2006.284
30. Picioreanu, C., Pérez, J., van Loosdrecht, M. C. M. (2016). Impact of cell cluster size on apparent half-saturation coefficients for oxygen in nitrifying sludge and biofilms. *Water Research*, *106*, 371–382. https://doi.org/10.1016/j.watres.2016.10.017
31. Piechna, P., Żubrowska-Sudoł, M. (2017). Respirometric activity of activated sludge and biofilm in IFAS-MBBR system. *Journal of Ecological Engineering*, *18*(4), 145–151. https://doi.org/10.12911/22998993/74604
32. Pochana, K., Keller, J. (1999). Study of factors affecting simultaneous nitrification and denitrification (SND). *Water Science and Technology*, *39*(6), 61–68. https://doi.org/10.2166/wst.1999.0262
33. Rittmann, B. E., McCarty, P. L. (2020). *Environmental biotechnology: Principles and applications* (2nd ed.). McGraw-Hill Education.
34. Sin, G., Guisasola, A., De Pauw, D. J. W., Baeza, J. A., Carrera, J., Vanrolleghem, P. A. (2005). A new approach for modelling simultaneous storage and growth processes for activated sludge systems under aerobic conditions. *Biotechnology and Bioengineering*, *92*(5), 600–613. https://doi.org/10.1002/bit.20741
35. Sirianuntapiboon, S., Jeeyachok, N., Larplai, R. (2005). Sequencing batch reactor biofilm system for treatment of milk industry wastewater. *Journal of Environmental Management*, *76*(2), 177–183. https://doi.org/10.1016/j.jenvman.2005.01.018
36. Tao, T., Chang, S. (2025). Simultaneous heterotrophic nitrification and aerobic denitrification of high C/N wastewater in a sequencing batch reactor. *Water*, *17*(17), 2515. https://doi.org/10.3390/w17172515
37. Third, K. A., Burnett, N., Cord-Ruwisch, R. (2003). Simultaneous nitrification and denitrification using stored substrate (PHB) as the electron donor in an SBR. *Biotechnology and Bioengineering*, *83*(6), 706–720. https://doi.org/10.1002/bit.10708
38. Wu, J., Wan, J., Yu, L., Zhang, M., Ducoste, J. J. (2021). The effect of activated sludge floc morphology on the measurement of biomass half-saturation coefficient: A 2D CFD biofilm model-based evaluation and experimental verification. *Biochemical Engineering Journal*, *168*, 107931. https://doi.org/10.1016/j.bej.2021.107931
39. Zawadzka, B., Siwiec, T., Marzec, M. (2021). Effectiveness of dairy and domestic wastewater treatment and technological reliability of the wastewater treatment plant in Michów, Poland. *Journal of Ecological Engineering*, *22*(10), 141–151. https://doi.org/10.12911/22998993/142117
40. Zhang, Y., Yin, Z., Liu, M., Liu, C. (2024). Enhancing simultaneous nitrification and denitrification in a plant-scale integrated fixed-film activated sludge system: Focusing on the cooperation between activated sludge and biofilm. *Chemical Engineering Journal*, *496*, 154322. https://doi.org/10.1016/j.cej.2024.154322